

C-V model of CdS/CdTe thin-film solar cells dependent on applied voltage frequency

P. A. Hernández-León and F. L. Castillo-Alvarado

*Escuela Superior de Física y Matemáticas, Instituto Politécnico Nacional, U.P.A.L.M.,
Lindavista 07738, Gustavo A. Madero, México City, México.*

A. González-Cisneros

*Escuela Superior de Computo, Instituto Politécnico Nacional,
Av. Juan de Dios Bátiz esq. Av. Miguel Othón de Mendizábal, Lindavista 07738, Gustavo A. Madero, México City, México.*

A. A. Durán-Ledezma

*SEPI, ESIME Ticomán, Instituto Politécnico Nacional,
Av. Ticomán No. 600, San José Ticomán, 07340, Gustavo A. Madero, México City, México.*

** e-mail: aduranl@ipn.mx,*

tel +52(55) 5729-6000 ext. 52052

tel. +52(55) 26996688

Received 02 December 2022; accepted 1 March 2023

In CdS/CdTe solar cells, the dependence on the frequency of the applied voltage is essential to improve theoretical results. Our model considers the conservation of energy and charge, a ternary layer, and the existence of plasmons at the interface. As a result, the capacitance depends on the frequency of the induced field in the heterojunction. Likewise, a plasmon at the interface on the surface semiconductor was formed. Finally, the findings provided with the theoretical model and the experimental data were compared, and a better adjustment was obtained.

Keywords: Solar cells; plasmons; heterojunction; capacitance.

DOI: <https://doi.org/10.31349/RevMexFis.69.041604>

1. Introduction

The cumulative capacity of solar photovoltaic power in the global markets continues to increase in popularity. From its optical, electronic, and chemical properties, CdS is considered the best-suited n-type heterojunction partner to CdTe for high efficiency and low cost, with a maximum theoretical efficiency of about 22.1% for such cells [1].

Photovoltaic science and technology have been improving simultaneously, and the development of their applications has been outstanding. In China, the total annual solar cell and module production capacity may increase from 361 GW at the end of last year to up to 600 GW at the end of 2022, according to the Asia Europe Clean Energy (solar) advisory. The cumulative worldwide capacity of solar photovoltaic power continues to increase [1, 2].

In 2020 there was a world record in efficiency obtained with solar cells manufactured with thin-film technology at 23.4% [3], and maximum efficiency of 22.1% in CdTe thin-film solar cells was recently reported [4]. CdTe is one of the best options for developing better and more efficient thin-film solar cells due to its excellent band gap (1.5eV) at room temperature, high absorption coefficient, very robust, and highly chemically stable [5]. On the scientific and technological side, excellent results have been achieved [6, 7]. Creating new ones and improving the existing materials for photo-

voltaic conversion has been one of the most studied areas in the last years [8, 9]. The plasmonic effect is a crucial ingredient for implementing most photovoltaic materials; this is responsible for the most exciting phenomena that such materials present, for instance, negative refractive index, superlensing, and cloaking [10, 11].

The surface plasmons phenomenology has recently been investigated in various systems [6, 12–15], which aim to optimize the trapping of photons and absorption processes. In addition, plasmons increase the capacity to generate electron-hole pairs, allowing higher performance. This phenomenon is present in the interfaces of semiconductor thin films. Therefore, its study is necessary to understand photovoltaic energy's gain or loss mechanisms to improve the efficiency of solar cells.

In this work, we were able to measure the solar cell capacitance by applying an alternating voltage of frequency ω , considering the system at room temperature. With these assumptions, it was possible to observe an increase of free charge carriers in each material that makes up the heterojunction; thus, we can consider the semiconductor as a cloud of electrons and holes [17, 18]. When the frequency increases, some properties of these materials change, such as the electric permittivity [19, 20]. We report a theoretical study based on the presence of plasmons in the interlayer, considering the frequency dependence of the applied voltage on the permittivity.

The Capacitance-Voltage (C-V) graph is compared with the experimental results of the CdS/CdTe solar cells and previous theoretical models. For instance, Castillo *et al.* [21, 22] consider in their model a direct voltage and a constant electrical permittivity; however, in the present report, an alternating voltage which is more consistent with the experimental conditions, and a dependence on the electrical permittivity with the frequency of the applied voltage is also assumed. As a result, we obtained a better fitting to the C-V graph experimental data by using these premises as well as consistency for values of the discontinuity band and interface charge density, respectively.

2. Theoretical method

2.1. Dependence of the dielectric permittivity when applying a variable electric field to a semiconductor

The theoretical model C-V for CdS/CdTe solar cells was improved as shown in Fig. 1. To obtain the relation of the dielectric permittivity with the frequency of the applied voltage during the experimental measurement process, it was considered the model of electron gas applying a positive background, where the charge density is given by $\rho_0 = n|e|$, where n is the number of electrons per unit of volume, and e is the fundamental electric charge.

If longitudinal waves are applied to the electron gas, dilatations and contractions appear, destroying the charge neutrality, and the presence of Coulomb restitution forces occurs. We obtained the plasmon dispersion relation [23]

$$\omega_k^2 = \omega_p^2 + \left(\frac{\alpha}{mn}\right) k^2, \quad (1)$$

with

$$\omega_p^2 = 4\pi \frac{ne^2}{m\epsilon_0}, \quad (2)$$

where ω_p is the plasma frequency, m the electron mass, and k the wave vector.

If $k = 0$ in Eq. (1), the displacement x of the electron gas is related to the polarization as

$$P = nex = -\frac{ne^2}{m\omega^2}. \quad (3)$$

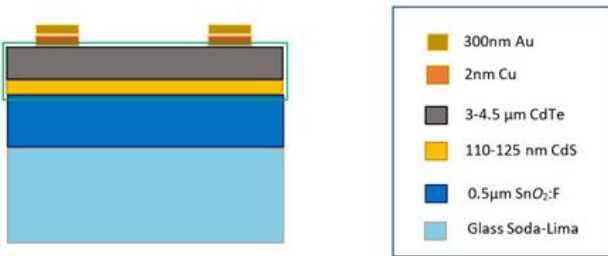


FIGURE 1. CdS / CdTe polycrystalline solar cell (second generation), where the CdS is used as window material and CdTe as the active material.

The dielectric permittivity can be written in terms of the electric susceptibility as

$$\epsilon_\tau = [1 + \chi], \quad (4)$$

where

$$\chi = \frac{P}{E}, \quad (5)$$

with P the polarization and E the electrical field.

Using Eqs. (3), (4), and (5), the frequency dependence is obtained for the electric permittivity as

$$\epsilon_\tau(\omega) = 1 + 4\pi \frac{P}{E} = 1 - \frac{4\pi ne^2}{m\omega^2} = 1 - \frac{\omega_p^2}{\omega^2}, \quad (6)$$

with this expression, we can consider the following cases

- If $\omega > \omega_p$, then $\epsilon(\omega) > 0$, which means that the wave propagates.
- If $\omega < \omega_p$, then $\epsilon(\omega) < 0$, which implies that the wave decays exponentially.

Since the field frequency is smaller than the CdS and the CdTe thin films plasma frequencies, the permittivity is negative [24].

2.2. Cardinal equations

Cardinal equations are usually applied to describe the electronic behavior of solar cell [17, 21, 25]. In the model proposed here, the presence of a ternary ($\text{CdS}_x\text{Te}_{1-x}$) in the heterojunction is considered, which appears during the p-n heterojunction fabrication, with $x = 0.75$ [6]. The ternary takes the place of an n-type semiconductor (CdS). To obtain the ternary stoichiometry, we use a linear combination of the CdS and CdTe parameters reported in the literature [26], consistent with those obtained previously [27, 28].

If a voltage (V_a) is applied in the heterojunction, loses equilibrium, and quasi-levels replace the Fermi levels, hence,

$$\begin{aligned} E_{F1} - E_{F2} - \Delta E_{V(\text{ternary})} - qV_a \\ = q[\varphi_{s2}(V_a) - \varphi_{s1}(V_a)], \end{aligned} \quad (7)$$

where E_{F1} and E_{F2} are the differences between the quasi-energy Fermi levels corresponding to CdTe and $\text{CdS}_x\text{Te}_{1-x}$ respectively. The interference potential of CdTe and the ternary are respectively given by $\varphi_{s2}(V_a)$ and $\varphi_{s1}(V_a)$. Also $\Delta E_{V(\text{ternary})}$ is the valence band of the ternary and V_a is the voltage applied at the p-n junction.

The respective valence band levels are given by

$$\begin{aligned} E_{FV1} = E_{Fn1} - E_{V1} = \frac{E_{g1}}{2} + \frac{3}{4}kT \ln \frac{m^*h1}{m^*e1} \\ + kT \ln \frac{N_d - N_a}{n_i} - q\varphi_{F1}, \end{aligned} \quad (8)$$

$$\begin{aligned} E_{FV2} = E_{Fp2} - E_{V2} = \frac{E_{g2}}{2} + \frac{3}{4}kT \ln \frac{m^*h2}{m^*e2} \\ + kT \ln \frac{N_d - N_a}{n_i} - q\varphi_{F2}. \end{aligned} \quad (9)$$

The separation of Fermi quasi-levels is given by

$$E_{Fn1} = E_{Fp2} + qV_a, \quad (10)$$

and the equation describing the charge neutrality is

$$Q_1[\varphi_{s1}(V_a)] + Q_2[\varphi_{s2}(V_a)] + q\sigma = 0, \quad (11)$$

where Q_1 and Q_2 are the non-equilibrium charges in the semiconductors, which are defined by

$$Q_j = \text{sign}[\varphi_{sj}(V_a)] \cdot \sqrt{2} \frac{\varepsilon_0 \varepsilon(\omega)_{sj}}{\beta L_{Dj}} \cdot e^{\frac{u_{-1}}{2}} \times (\varphi_{sj}(V_a) \cdot \sinh[u_{+j}] + \cosh[u_{+j} - u_{sj}(V_a)] - \cosh[u_{+j}])^{1/2}. \quad (12)$$

with $j = 1, 2$. Here $u_{+} = (\beta[\varphi_{F1} + \varphi_{F2}])/2$, $\beta = q/kT$ and the sign depends on the value of u , then

$$\text{sign}(u) = \begin{cases} +1, & u < 0 \\ -1, & u > 0 \end{cases}. \quad (13)$$

There are an equal number of positive and negative charges in the interface of the materials where the space charge region behaves like a parallel plates capacitor, so the third cardinal equation considered is

$$\frac{1}{\text{CdTe/CdS}_x\text{Te}_{1-x}} = \frac{1}{C_1[\varphi_{s1}(V_a)]} + \frac{1}{C_2[\varphi_{s2}(V_a)]}, \quad (14)$$

where

$$C_j = \frac{(\varepsilon_0 \varepsilon(\omega)_{sj})^2}{\beta L_{Dj}^2 Q_j} \cdot e^{\frac{u_{-1}}{2}} [\sinh[u_{+j}] - \sinh[u_{+1} - u_{s1}(V_a)]] = \frac{q \varepsilon_0 \varepsilon(\omega)_{sj}}{Q_j} \times [N_j + 2Nn_{ij} \cdot e^{\frac{u_{-1}}{2}} \sinh[u_{+j} - u_{sj}(V_a)]], \quad (15)$$

$j = 1, 2.$

In the previous equation, C_1 and C_2 are related to the capacitors formed by the ternary and CdTe layers, respectively.

3. Results

Using Eqs. (2) and (6), the electrical permittivity and the plasma frequency for each semiconductor were determined

(see Table I). The permittivity values obey the dispersion relation in Eq. (6) for a wave vector close to the plasma frequency. The fact that the values of the plasma frequency ω_p are less than the frequency ω makes the permittivity negative, causing the waves to be reflected and preventing them from propagating in the medium. Semiconductors, especially CdS and CdTe, have low densities of free carriers, so the plasma frequency is between the mid and near-infrared [29].

The Capacitance Voltage technique was used to compare the theoretical results with the experimental ones and determine the heterojunction's physical properties. The C-V measurements were done at a frequency of 0.1 MHz from 0 to 40 mV. From Eqs. (7) and (14), the capacitance values have been obtained by varying the voltage in 0.05mV intervals. The parameters used in the calculation are based on the experimental data and parameters reported in previous works [21, 22, 26]. Figure 2 compares the experimental data (black spheres), the theoretical values considering only one ternary layer (Castillo *et al.* red spheres), and the theoretical results our model predict (blue spheres).

A Schottky barrier in the contacts exists for the applied voltage from 0 to 19 mV, inducing a non-ohmic behavior. So, there is a significant disagreement between theory and experiment in that voltage range. Furthermore, fitting the ex-

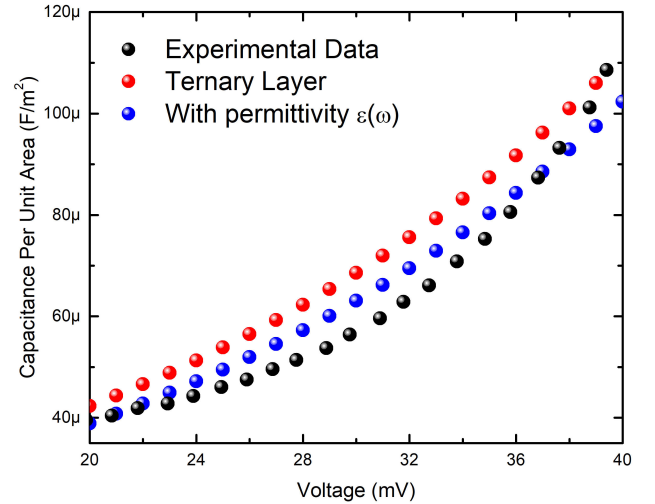


FIGURE 2. C-V plot. Comparison of experimental data (black spheres), interface ternary layer (red spheres), and the consideration of plasmon effect in permittivity (blue spheres).

TABLE I. Frequency of the applied voltage ω , electric permittivity ε_r , frequency dependent electrical permittivity $\varepsilon_r(\omega)$ and the plasma frequency of the CdS and CdTe thin films.

	Experimental	Literature [26]	Theoretical results	
	Applied voltage frequency ω (Mhz)	Electric permittivities ε_r	Electric permittivities ω_p (Mhz)	Plasma frequency $\varepsilon_r(\omega)$
CdS	0.1	9.12	0.292	7.5
CdTe	0.1	10.2	0.326	9.6

perimental data allows getting the valence band discontinuity value of $\Delta E_v = 0.89$ eV and the interface charge density $\sigma = 1 \times 10^{13} \text{ m}^{-2}$ results consistent with those previously obtained [21]

4. Conclusions

Our results offer insight into understanding physical phenomena involved in semiconductor interfaces; such findings could provide tools for improving solar cells. Considering the frequency of the alternating incoming voltage, we found that plasmons in the interface are formed with a plasma frequency greater than the frequency of the applied voltage, which makes a negative permittivity; thus, electromagnetic waves are reflected and therefore decay exponentially

in space. Moreover, the plasmons frequency found is in the infrared region, hence the plasmon does not affect the solar cell efficiency. The capacitance versus the applied voltage of CdS/CdTe thin-film solar cells has been calculated. Comparing to previously reported theoretical results where frequency dependency over the electric permittivity is not considered, a better fitting with our model is achieved.

Acknowledgment

This work was partially supported by COFAA-IPN, EDD-IPN, EDI-IPN, Sistema Nacional de Investigadores (SNI-CONACYT) and Instituto Politécnico Nacional (SIP-IPN Project Numbers 20220573, 20221817 and 20221554).

1. <https://www.nrel.gov/pv/cell-efficiency.html>.
2. <https://www.pv-magazine.com/2022/10/24/chinas-solar-cell-production-capacity-may-reach-600-gw-by-year-end/>.
3. M. Powalla *et al.*, Thin-film solar cells exceeding 22% solar cell efficiency: An overview on CdTe-, Cu (In, Ga) Se2-, and perovskite-based materials. *Applied Physics Reviews*, **5** (2018) 041602. <https://doi.org/10.1063/1.5061809>.
4. Q. Fu *et al.*, Recent progress on the long-term stability of perovskite solar cells. *Adv. Sci.*, **5** (2018) 1700387. <https://doi.org/10.1002/advs.201700387>.
5. T. Sinha, D. Lilhare, and A. Khare, A review on the improvement in performance of CdTe/CdS thin-film solar cells through optimization of structural parameters. *J. Mater. Sci.*, **54** (2019) 12189, <https://doi.org/10.1007/s10853-019-03651-0>.
6. T. M. Mazur, V. V. Prokopiv, M. P. Mazur, and U. M. Pysklynets, Solar cells based on CdTe thin films. *Phys. Chem. Solid State*, **22** (2021) 817, <https://doi.org/10.15330/pcss.22.4.817-827>.
7. A. Romeo, and E. Artagiani, CdTe-based thin film solar cells: past, present and future. *Energies*, **14** (2021) 1684. <https://doi.org/10.3390/en14061684>.
8. Y. Liu *et al.*, Recent progress in organic solar cells (Part I material science). *Sci. China Chem.* **65** (2022) 224, <https://doi.org/10.1007/s11426-021-1180-6>.
9. Y. Zhao, L. Yu, and M. Sun, Recent progress in emerging 2D layered materials for organic solar cells. *Sol. Energy*, **218** (2021) 621, <https://doi.org/10.1016/j.solener.2021.02.066>.
10. A. J. Hoffman *et al.*, Negative refraction in semiconductor metamaterials. *Nature materials*, **6** (2007) 946, <https://doi.org/10.1038/nmat2033>.
11. S. A. Maier, Plasmonics: fundamentals and applications Vol. 1 (Springer 2007) p. 245.
12. K. Kluczyk, C. David, J. Jacak, and W. Jacak, On modeling of plasmon-induced enhancement of the efficiency of solar cells modified by metallic nano-particles. *Nanomaterials* **9** (2018) 3, <https://doi.org/10.3390/nano9010003>.
13. D. T. Gangadharan, Z. Xu, Y. Liu, and R. Izquierdo, and D. Ma, Recent advancements in plasmon-enhanced promising third-generation solar cells. *Nanophotonics*, **6** (2017) 153, <https://doi.org/10.1515/nanoph-2016-0111>.
14. G. Liu, Y. Lou, Y. Zhao, and C. Burda, Directional Damping of Plasmons at Metal-Semiconductor Interfaces. *Acc. Chem. Res.*, **55** (2022) 1845, <https://doi.org/10.1021/acs.accounts.2c00001>.
15. S. Kim, J. Suh, T. Kim, J. Hong, and S. Cho, Plasmon-enhanced performance of CdS/CdTe solar cells using Au nanoparticles. *Opt. Express* **27** (2019) 22017, <https://doi.org/10.1364/OE.27.022017>.
16. T. S. Luk, N. T. Fofang, J. L. Cruz-Campa, I. Frank, and S. Campione, Surface plasmon polariton enhanced ultrathin nanostructured CdTe solar cell. *Opt. Express*, **22** (2014) A1372, <https://doi.org/10.1364/OE.22.0A1372>.
17. N. W. Ashcroft, Solid state physics, 1st ed. (Harcourt College Publishers,1976) pp. 402, 512-517, 589-609.
18. H. Mathieu, H. Fanet, Física de semiconductores y componentes eléctricos, 1ra ed. (Universidad Nacional Autónoma de México, 2013), pp. 94-95
19. M. Flores *et al.*, Microwire composite electromagnetic parameters extraction by waveguide measurements at X-band. *J. Electromag. Waves Appl.*, **28** (2013) 202, <https://doi.org/10.1080/09205071.2013.862186>.
20. U. Kaatz, Techniques for measuring the microwave dielectric properties of materials. *Metrologia*, **47** (2010) S91. <https://doi.org/10.1088/0026-1394/47/2/S10>.
21. F. L. Castillo-Alvarado, *et al.*, C-V calculations in CdS/CdTe thin films solar cells. *Thin Solid Films*, **518** (2010) 1796, <https://doi.org/10.1016/j.tsf.2009.09.035>.
22. A. Gonzalez-Cisneros, F. L. Castillo-Alvarado, J. Ortiz-Lopez, and G. Contreras-Puente, CV Calculations in CdS/CdTe Thin

- Films Solar Cells with a CdS_xTe_{1-x} Interlayer. *International Journal of Photoenergy*. (2013). <https://dx.doi.org/10.1155/2013/513217>.
23. C. Kittel, Quantum Theory of Solids, 1st ed. (John Wiley & Sons, 1963), pp. 34-37
 24. W. Sun, L. Li, J. Zhang, and H. Yin, Theoretical and Experimental Study on Dielectric Constant of Cadmium Telluride in Terahertz Band. *Procedia Computer Science*, **174** (2020) 667, <https://doi.org/10.1016/j.procs.2020.06.140>.
 25. K. V. E. Shalimova, Física de los Semiconductores (Mir, 1975), pp. 24-32, 71-101.
 26. G. Chiarotti and P. Chiaradia (eds.), Physics of Solid Surfaces, Vol. 45B, 1st ed. (Springer, 2018), pp. 1120-1124.
 27. I. Biziz, El-H. Atmani, N. Fazouan, and M. Aazi, First-principles calculations of structural, electronic and optical properties of CdTe_xS_{1-x} and Cd_{1-x}Zn_xS ternary alloys, *Surf. Interfaces* **24** (2021) 101126, <https://doi.org/10.1016/j.surfin.2021.101126>.
 28. B. G. Mendis, Q. M. Ramasse, T. P. Shalvey, J. D. Major, and K. Durose, Optical properties and dielectric functions of grain boundaries and interfaces in CdTe thin-film solar cells. *ACS Appl. Energy Mater.* **2** (2019) 1419, <https://doi.org/10.1021/acsaem.8b01995>.
 29. H. G. Castro Lora, Estudio de las propiedades ópticas y estructurales en películas delgadas de ZnSe, M.Sc. Thesis, Universidad Nacional de Colombia, 2013, pp. 25-27.